A R C H I V E O F M E C H A N I C A L E N G I N E E R I N G

VOL. LXV 2018 Number 3

DOI: 10.24425/124490

Key words: third-grade viscoelastic fluid model, thermal jump, entropy generation, Bejan number, Hartmann number

K. MADHAVI [1], *V. RAMACHANDRA PRASAD* [2], *S. ABDUL GAFFAR* [3], *K. VENKATADRI* [4]

ENTROPY ANALYSIS OF THIRD-GRADE MHD CONVECTION FLOWS FROM A HORIZONTAL CYLINDER WITH SLIP

In thermosfluid dynamics, free convection flows external to different geometries, such as cylinders, ellipses, spheres, curved walls, wavy plates, cones, etc., play major role in various industrial and process engineering systems. The thermal buoyancy force associated with natural convection flows can play a critical role in determining skin friction and heat transfer rates at the boundary. In thermal engineering, natural convection flows from cylindrical bodies has gained exceptional interest. In this article, we mathematically evaluate an entropy analysis of magnetohydrodynamic *third-grade* convection flows from permeable cylinder considering velocity and thermal slip effects. The resulting non-linear coupled partial differential conservation equations with associated boundary conditions are solved with an efficient unconditionally stable implicit finite difference Keller-Box technique. The impacts of momentum and heat transport coefficients, entropy generation and Bejan number are computed for several values of non-dimensional parameters arising in the flow equations. Streamlines are plotted to analyze the heat transport process in a two-dimensional domain. Furthermore, the deviations of the flow variables are compared with those computed for a Newtonian fluid and this has important implications in industrial thermal material processing operations, aviation technology, different enterprises, energy systems and thermal enhancement of industrial flow processes.

Nomenclature

a	radius of the cylinder
Be	non-dimensional Bejan number

[1] *Department of Mathematics, Madanapalle Institute of Technology and Science, Madanapalle – 517325, India. Email: seshadri.madhavi@gmail.com*

[2] *Department of Mathematics, School of Advanced Sciences, VIT University, Vellore – 632014, Tamil Nadu, India. Email: v.ramachandraprasad@vit.ac.in*

[3] *Department of Mathematics, Salalah College of Technology, Salalah, Oman. Email: abdulsgaffar@gmail.com*

[4] *Department of Mathematics, Vemu Institute of Technology, P. Kothakota, India. Email: venkatadri.venki@gmail.com*

B_0 constant imposed magnetic field
Br Brinkman number
C_f skin friction coefficient
f dimensionless stream function
g gravitational acceleration
Gr Grashof number
Ha Hartmann number
I identity tensor
k thermal conductivity of the fluid
K_0 thermal slip factor
M magnetic parameter
N_0 velocity slip factor
N_G entropy generation number
Nu heat transfer coefficient
Pr Prandtl number
p pressure
Re Reynolds number
T fluid temperature
$u,\ v$ dimensionless velocity components in x and y directions respectively
V velocity vector
x stream wise coordinate
y transverse coordinate

Greek symbols

Ω dimensionless heat function
α thermal diffusivity
β coefficient of thermal expansion
τ extra stress tensor
Φ azimuthal coordinate
σ electric conductivity of the fluid
η dimensionless radial coordinate
μ dynamic viscosity
ξ non-dimensional tangential coordinate
ψ non-dimensional stream function
ν kinematic viscosity
ε_1 first viscoelastic material fluid parameter
ε_2 second viscoelastic material fluid parameter
ρ fluid density
β_3 third grade material parameter

θ non-dimensional temperature

φ dimensionless third grade viscoelastic fluid parameter

Subscripts

w conditions on the wall

∞ free stream condition

1. Introduction

In many fluids, the flow properties are difficult to explain by a single constitutive equation like Newtonian model. Geological materials and polymer solutions used in different industries and engineering processes are such fluids which cannot be explained by Newtonian model. The materials that cannot be explained using Newtonian model are called the Non-Newtonian fluid models. In the past, several decades non-Newtonian transport phenomena have motivated considerable interest among engineers, physicists and mathematicians. This area presents a rich spectrum of nonlinear boundary value problems largely due to the extremely diverse range of rheological models available for simulating complex flow behavior. In such fluids, the shear stress and strain rate relation is non-linear. The non-Newtonian fluid models are arduous [1]. The popular non-Newtonian models include oblique micropolar flows [2], Walter's-B fluids [3], Jeffrey's flows [4], Williamson fluid [5], nanofluid [6], Maxwell flows [7], Eyring–Powell flows [8], tangent hyperbolic flows [9], Oldroyd-B fluid [10] and Power-law fluid [11]. A particular group of viscoelastic fluids is simulated with the *third-grade model*. Examples include cooling oil, polymer solutions and molten polymers in chemical engineering. Of the different non-Newtonian fluids discussed in the literature, the differential, integral and rate type models gained prominence. The third-grade model has the ability to predict shear thinning and thickening characteristics of the fluid. In ref. [12], the authors presented the flow and heat transport of radiative third-grade model in the presence of Ohmic dissipation. Ref. [13] presents the radiative magnetohydrodynamic third grade flow model from an isothermal cone. The author of [14] presented the heat transfer analysis of third grade model past parallel plates. Recent studies with regards to third grade fluid include [15–20].

The presence of magnetic field in natural convection flows plays an important role and has many applications like nuclear reactor cooling, magnetohydrodynamic (MHD) generators, geophysics, astrophysics, aerodynamics, plasma engineering, exploration of oil, etc. The MHD convection flow of Jeffrey's fluid was considered in [21]. A spectral relaxation method was employed in [22] to study unsteady MHD flows past a semi-infinite vertical plate. Authors of [23] discussed the MHD convection flows of nanofluid over an exponential permeable stretching sheet using R-K method. In ref. [24] authors studied the entropy analysis of magnetohydrodynamic electroosmotic flow. Other recent studies on MHD include [9, 25–29].

The effective utilization of energy and ideal utilization of resources has persuaded investigate into enhancing the productivity of mechanical procedures. Research on the enhancement in heat exchange as a standout amongst the most compelling elements in energy consumption has been the fundamental core interest. Assessment of entropy generation and the utilization of unique fluid like non-Newtonian fluids are essential and proficient strategies for accomplishing ideal warmth exchange. Entropy production determines the irreversibility related with the natural process such as counter flow heat exchanger for gas to gas applications [30]. Resent applications of entropy generation include pseudo-optimization design processes for solar heat exchangers, solar energy collectors and heat energy systems. Minimization of entropy generation has emerged as a fundamental modern technique for designing thermal systems. In [31] authors presented the entropy generation of fourth-grade fluid using perturbation method. Ref. [32] presents the entropy generation of MHD convection flows of third-grade fluid past a stretching sheet. The entropy generation of magnetohydrodynamic flows of viscoelastic fluid past a stretching surface in the presence of Joule dissipation, viscous dissipation and Darcy dissipation and heat generation was investigated in [33]. In [34], the authors addressed the entropy generation minimization of nonlinear radiative mixed convection flow analysis from a stretching sheet. The Maxwell's thermal conductivity model to study the entropy generation of mixed convection peristaltic flow of methanol nanofluid was proposed in [35]. The authors of [36] employed homotopy analysis method to study the nonlinear radiative EMHD Nanofluid flows from a stretching sheet. In ref. [37], the authors analyzed the entropy analysis of Casson fluid flow with slip effects.

The effects of slip are compelling in different thermal industry processes and manufacturing fluid dynamic systems such as fluid transportation, material processing and rheometric measurements. In general, velocity slip elevates the heat transfer whereas thermal jump reduces the heat transfer. The slip conditions were first presented in [38]. Ref. [39] analyzes the entropy generation through porous annulus with slip and convective condition. Authors of [40] presented the nonlinear radiative magnetohydrodynamic flow of nanofluid considering velocity slip, viscous dissipation and Joule heating. In Ref. [41], the authors examined the slip effects of unsteady MHD squeezing flows using homotopy perturbation method. The Chebyshev spectral collocation method to explore the convective and slip effects of micropolar fluid through porous channel in [42]. Further studies include [27, 43, 44].

To the authors' knowledge, no studies have been communicated with regard to *viscoelastic MHD convection flow of permeable horizontal circular cylinder* with slip conditions. In the present study, non-similarity mathematical analysis is presented for steady MHD flows in viscoelastic fluid from permeable horizontal circular cylinder with slip effects. The Keller-box differences scheme is employed to solve the normalized boundary layer equations and the effects of third-grade fluid parameter (φ), material fluid parameters ($\varepsilon_1, \varepsilon_2$), velocity slip ($S_f$), thermal

jump (S_T), magnetic parameter (M) on the relevant flow variables are described in detail. Also, the influence of Reynolds number, Hartmann number, Brinkman number and dimensionless heat function and other physical parameter on entropy generation and Bejan number are presented. The present study finds application in solar film collectors, heat exchanger technology, geothermal energy storage systems, etc.

2. Third-grade viscoelastic fluid model

A subclass of non-Newtonian fluid model considered in the present study is the third-grade fluid owing to its simplicity. The model precisely catches the viscoelastic qualities of specific polymers [45, 46]. The Cauchy stress tensor of the third-grade viscoelastic model in view of [47] takes the form:

$$\tau = -pI + \mu A_1 + \alpha_1 A_2 + \alpha_2 A_1^2 + \beta_1 A_3 + \beta_2 (A_1 A_2 + A_2 A_1) + \beta_3 \left(\mathrm{tr} A_1^2\right) A_1 , \quad (1)$$

where A_i $(i = 1, 2, 3)$ are first Rivlin-Ericksen tensors [39] and are given by:

$$A_1 = (\nabla V) + (\nabla V)^{\mathrm{T}}, \quad (2)$$

$$A_n = \frac{\mathrm{d}A_{n-1}}{\mathrm{d}t} + A_{n-1}(\nabla V) + A_{n-1}(\nabla V)^{\mathrm{T}}; \qquad n > 1, \quad (3)$$

and α_j $(j = 1, 2)$ and β_k $(k = 1, 2, 3)$ are the material constants.

The steady, laminar, double-diffusive, incompressible, electrically-conducting, MHD convection flows of viscoelastic third-grade model from horizontal permeable cylinder is considered, as illustrated in Fig. 1). A magnetic field, B_0 is assumed to be directed normal to surface of the cylinder. The x and y axes are considered along the circumference and normal to surface of the cylinder respectively. Let $\Phi = x/a$ be the angle made by the y-axis with respect to the vertical, where $0 \leqslant \Phi \leqslant \pi$. The acceleration due to gravity g, is assumed to act downwards.

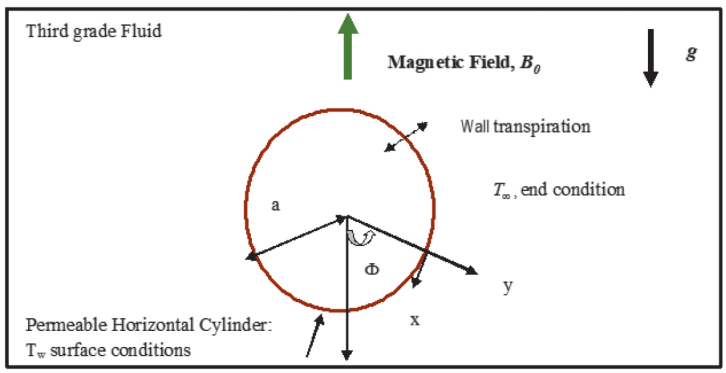

Fig. 1. Geometric illustration of the problem

Boussineq approximation is also assumed to holds. Let T_w be the constant temperature of the cylinder and the fluid and let T_∞ be the ambient temperature of the fluid. In line with the authors of [13–16], the boundary layer approximations for continuity, momentum and energy are given by:

$$\frac{\partial u}{\partial x} + \frac{\partial v}{\partial y} = 0, \tag{4}$$

$$\begin{aligned} u\frac{\partial u}{\partial x} + v\frac{\partial u}{\partial y} = \nu\frac{\partial^2 u}{\partial y^2} + \frac{\alpha_1}{\rho}\left[u\frac{\partial^3 u}{\partial x \partial y^2} + v\frac{\partial^3 u}{\partial y^3} + \frac{\partial u}{\partial x}\frac{\partial^2 u}{\partial y^2}\right] \\ + \frac{1}{\rho}\left[3\alpha_1 + 2\alpha_2\right]\frac{\partial u}{\partial y}\frac{\partial^2 u}{\partial x \partial y} \\ + \frac{6\beta_3}{\rho}\left(\frac{\partial u}{\partial y}\right)^2\frac{\partial^2 u}{\partial y^2} + g\beta\left(T - T_\infty\right)\sin\left(\frac{x}{a}\right) - \frac{\sigma B_0^2}{\rho}u, \end{aligned} \tag{5}$$

$$u\frac{\partial T}{\partial x} + v\frac{\partial T}{\partial y} = \alpha\frac{\partial^2 T}{\partial y^2}. \tag{6}$$

The boundary conditions are defined as:

$$\begin{array}{llllll} At & y = 0, & u = N_0\dfrac{\partial u}{\partial y}, & v = 0, & T = T_w + K_0\dfrac{\partial T}{\partial y}, \\ As & y \to \infty, & u \to 0, & v \to 0, & T \to T_\infty. \end{array} \tag{7}$$

If $N_0 = 0 = K_0$, then no-slip case arises. Defining the stream function, ψ as $u = \dfrac{\partial \psi}{\partial y}$ and $v = -\dfrac{\partial \psi}{\partial x}$ Eq. (4) is satisfied. The dimensionless variables considered are:

$$\begin{array}{llll} \xi = \dfrac{x}{a}, & \eta = \dfrac{y}{a}\mathrm{Gr}^{1/4}, & \psi = \nu\sqrt[4]{\mathrm{Gr}_x}\,\xi f, & \theta(\xi,\eta) = \dfrac{T - T_\infty}{T_w - T_\infty}, \\ \varphi(\xi,\eta) = \dfrac{C - C_\infty}{C_w - C_\infty}, & \mathrm{Pr} = \dfrac{\nu}{\alpha}, & \mathrm{Gr} = \dfrac{g\beta(T_w - T_\infty)a^3}{\nu^2}, & \\ \varphi = \dfrac{\beta_3\nu}{\rho a^4}\mathrm{Gr}^{3/2}, & \varepsilon_1 = \dfrac{\alpha_1}{\rho a^2}\mathrm{Gr}^{1/2}, & \varepsilon_2 = \dfrac{\alpha_2}{\rho a^2}\mathrm{Gr}^{1/2}, & \\ M = \dfrac{\sigma B_0^2 a^2}{\rho\nu\sqrt{\mathrm{Gr}}}, & S_f = \dfrac{N_0\mathrm{Gr}^{1/4}}{a}, & S_T = \dfrac{K_0\mathrm{Gr}^{1/4}}{a}. & \end{array} \tag{8}$$

Using Eqn. (8), Eqns. (6) and (7) reduce as follows:

$$f''' + ff'' - (f')^2 + \varepsilon_1 \left[2f'f''' - ff^{iv}\right] + (3\varepsilon_1 + 2\varepsilon_2)(f'')^2 + 6\varphi\xi^2 (f'')^2 f''' + \theta\frac{\sin\xi}{\xi} - Mf'$$
$$= \xi\left[f'\frac{\partial f'}{\partial\xi} - f''\frac{\partial f}{\partial\xi} - \varepsilon_1\left(f'\frac{\partial f'''}{\partial\xi} + f'''\frac{\partial f'}{\partial\xi} - f^{iv}\frac{\partial f}{\partial\xi}\right) - (3\varepsilon_1+2\varepsilon_2) f''\frac{\partial f''}{\partial\xi}\right], \quad (9)$$

$$\frac{\theta''}{\mathrm{Pr}} + f\theta' = \xi\left(f'\frac{\partial\theta}{\partial\xi} - \theta'\frac{\partial f}{\partial\xi}\right). \quad (10)$$

The transformed dimensionless boundary conditions are:

$$\begin{aligned} &At \quad \eta = 0, \qquad f = 0, \qquad f' = S_f f''(0), \qquad \theta = 1 + S_T\theta'(0), \\ &As \quad \eta \to \infty, \qquad f' \to 0, \qquad f'' \to 0, \qquad \theta \to 0. \end{aligned} \quad (11)$$

The shear stress C_f and heat transfer rate are defined as

$$C_f = \xi f''(\xi,0) + \varepsilon_1 (2f'(\xi,0)f''(\xi,0) - f(\xi,0)f'''(\xi,0)) + 2\varphi (f''(\xi,0))^3, \quad (12)$$

$$\mathrm{Nu} = -\theta'(\xi,0). \quad (13)$$

3. Entropy generation analysis

The entropy generation due to MHD convection of third-grade fluid flows from a horizontal circular cylinder is discussed in this section. The volumetric rate of entropy generation due to magnetic field with heat transfer is given as:

$$S'''_{gen} = \frac{k}{T_\infty^2}\left(\frac{\partial T}{\partial y}\right)^2 + \frac{\mu}{T_\infty}\left(\frac{\partial u}{\partial y}\right)^2 + \frac{\sigma B_0^2}{T_\infty}u^2. \quad (14)$$

The 1st term on the right of eqn. (14) signifies the entropy produced by heat flow, the second term denotes the entropy due to viscous dissipation and the final term denotes the entropy due to the Lorentz force. The non-dimensional entropy heat generation N_G, the ratio of volumetric rate of entropy generation to characteristic entropy heat generation rate.

$$N_G = \frac{S'''_{gen}}{S'_0}\left(\frac{\frac{k}{T_\infty^2}\left(\frac{\partial T}{\partial y}\right)^2 + \frac{\mu}{T_\infty}\left(\frac{\partial u}{\partial y}\right)^2 + \frac{\sigma B_0^2}{T_\infty}u^2}{\frac{k(\Delta T)^2}{l^2 T_\infty^2}}\right), \quad (15)$$

$$N_G = \mathrm{Re}\,\theta'^2 + \frac{\mathrm{Br}}{\Omega}\mathrm{Re}\,\xi^2 f''^2 + \frac{\mathrm{Br}}{\Omega}\mathrm{Ha}^2\xi^2 f'^2, \tag{16}$$

where

$$\mathrm{Re} = \frac{l^2\mathrm{Gr}^{1/2}}{a^2}, \qquad \mathrm{Br} = \frac{\mu u^2}{k\Delta T}, \qquad \mathrm{Ha} = B_0 l\sqrt{\frac{\sigma}{\mu}},$$

$$\Omega = \frac{\Delta T}{T_\infty} \qquad \text{and} \qquad u = \frac{\nu}{a^2}\mathrm{Gr}^{1/2}\xi.$$

Eqn. (16) can be written as, $N_G = N_1 + N_2$, where $N_1 = \mathrm{Re}\,\theta'^2$ and $N_2 = \frac{\mathrm{Br}}{\Omega}\mathrm{Re}\,\xi^2 f''^2 + \frac{\mathrm{Br}}{\Omega}\mathrm{Ha}^2\xi^2 f'^2$ are respectively the irreversibility due to heat transfer and viscous dissipation.

The irreversibility is accessed via Bejan number (Be), is given by

$$\mathrm{Be} = \frac{N_1}{N_1 + N_2}. \tag{17}$$

Clearly, $0 \leqslant \mathrm{Be} \leqslant 1$. Therefore, if $\mathrm{Be} = 0$, N_2 dominates N_1 and vice versa if $\mathrm{Be} = 1$. And, if $\mathrm{Be} = 0.5$, the fluid friction contribution in entropy generation and the irreversibility due to heat transfer are equal, *i.e.*, $N_1 = N_2$.

4. Interpretation of results

The Keller-Box implicit difference scheme, elaborated in [48], is used to solve the nonlinear boundary value problem defined by Eqns. (9)–(10) along with boundary conditions (11). This is a very powerful technique for parabolic boundary flows. The method is very stable and achieves exceptional accuracy [48]. Recently applications of this method include hydromagntic Sakiadis flows [49], nanofluid transport from wedge [50], radiative rheological flows [51], water hammer modelling [52], porous media convection [53] and viscoelastic flows from semi-infinite vertical plate [4]. The discrete calculus of Keller-Box technique is fundamentally different from other numerical techniques. Very comprehensive solutions are obtained and are presented in Figs. 2–11. These figures illustrate profiles of velocity and temperature for different values of the thermophysical parameters, viz., φ, ε_1, ε_2, S_f, S_T, M, Re, Br, Ha, Pr and Ω. The default values of for these parameters are: $\varphi = 0.1$, $\varepsilon_1 = 0.3 = \varepsilon_2$, $S_f = 0.5$, $S_T = 1.0$, $M = 0.5$, $\mathrm{Re} = 5.0$, $\mathrm{Br} = 5.0$, $\mathrm{Ha} = 1.0$, $\Omega = 1.0$, $\mathrm{Pr} = 7.0$ and $\xi = 1.0$. The accuracy of the present code is validated and presented in Table 1 by comparing the present results of heat transfer rate with those of the authors [54] and [55] for different values of ξ and these are found to be in good correlation.

Fig. 2 illustrates the distributions of velocity (f'), temperature (θ) and entropy generation (N_G) for increasing third-grade material fluid parameter (φ). A significant decrease (Fig. 2a) in velocity is observed near the cylinder surface with

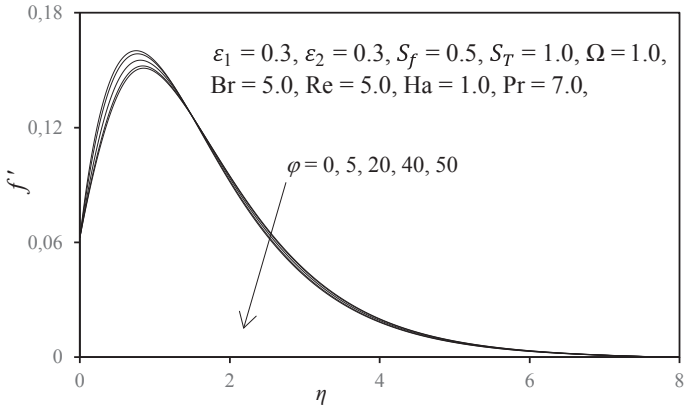

(a) Influence of φ_1 on velocity profiles

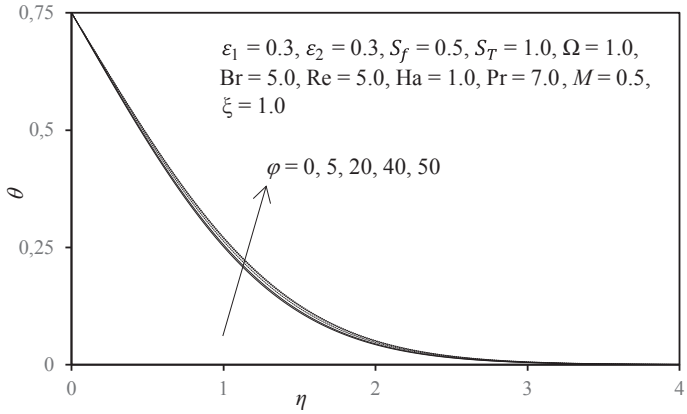

(b) Influence of φ_1 on temperature profiles

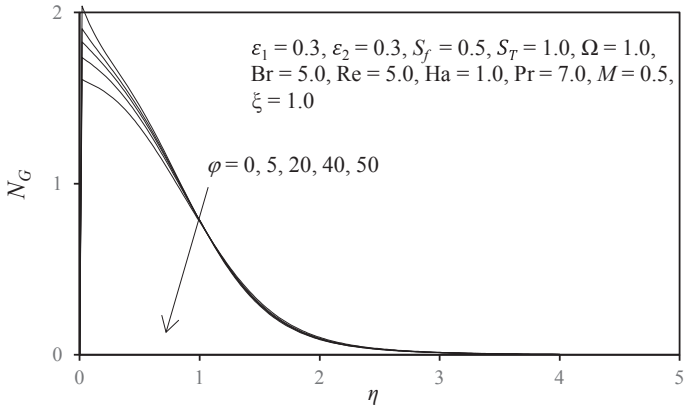

(c) Influence of φ_1 on entropy generation number

Fig. 2. Influence of φ on various parameters

Table 1.
Values of the local heat transfer coefficient (Nu) for various values of ξ with Pr = 0.71, $\varphi = \varepsilon_1 = \varepsilon_2 = \beta_3 = 0.0$, $S_f = S_T = 0$, $M = 0.5$

ξ	$\mathrm{Nu}\,\mathrm{Gr}^{-1/4} = -\theta'(\xi, 0)$		
	Merkin [54]	Yih [55]	Present
0.0	0.4212	0.4214	0.4215
0.2	0.4204	0.4207	0.4209
0.4	0.4182	0.4184	0.4188
0.6	0.4145	0.4147	0.4149
0.8	0.4093	0.4096	0.4101
1.0	0.4025	0.4030	0.4032
1.2	0.3942	0.3950	0.3953
1.4	0.3843	0.3854	0.3859
1.6	0.3727	0.3740	0.3746
1.8	0.3594	0.3608	0.3609
2.0	0.3443	0.3457	0.3459
2.2	0.3270	0.3283	0.3284
2.4	0.3073	0.3086	0.3088
2.6	0.2847	0.2860	0.2862
2.8	0.2581	0.2595	0.2597
3.0	0.2252	0.2267	0.2265
π	0.1963	0.1962	0.1965

increasing φ. The third-grade fluid model reduces to the well-known Newtonian model as $\varphi \to 0$, $\varepsilon_1 \to 0$ and $\varepsilon_2 \to 0$, viz:

$$f''' + ff'' - (f')^2 + \theta\frac{\sin\xi}{\xi} - Mf' = \xi\left[f'\frac{\partial f'}{\partial \xi} - f''\frac{\partial f}{\partial \xi}\right]. \tag{18}$$

However, thermal boundary layer is slightly increased for φ values. The third-grade fluid parameter (φ) is directly proportional to β_3 and inversely proportional to ν. An increase in φ is found to increase the temperature slightly (Fig. 2b). In Fig. 2c with increasing φ, the dimensionless entropy generation number decreases closer towards the walls. As φ increases, the bounding between the fluid particles becomes very strong making the fluid more viscoelastic.

Fig. 3 presents the distributions of velocity (f'), temperature (θ) and entropy generation number (N_G) for the increasing values of ε_1. The parameter, ε_1 appears in many terms in Eqn. (9) and is directly proportional to α_1. The velocity is seen

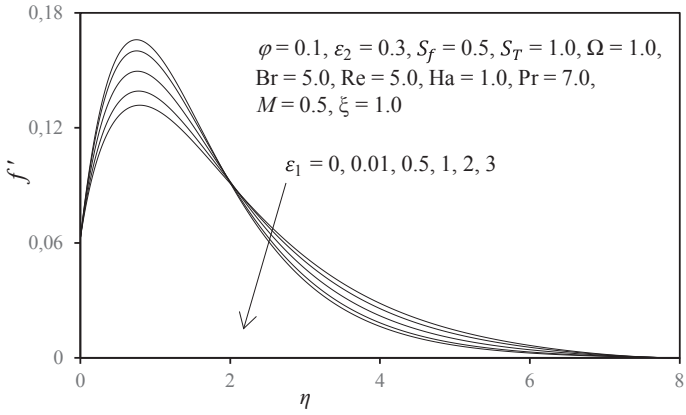

(a) Influence of ε_1 on velocity profiles

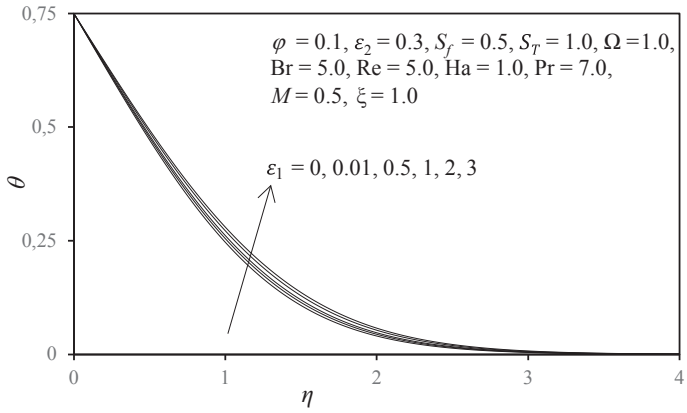

(b) Influence of ε_1 on temperature profiles

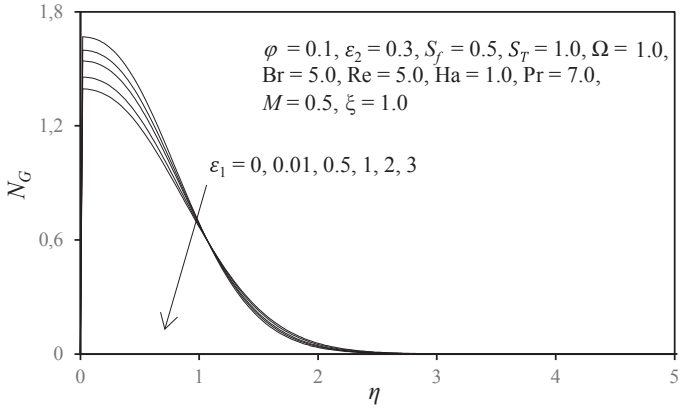

(c) Influence of ε_1 on entropy generation number

Fig. 3. Influence of ε_1 on various parameters

to decrease with increasing ε_1 values (Fig. 3a). The decreasing trend is due to the relaxation effect in the fluid further away from the cylinder surface which results in shear-thickening and higher viscosity in the fluid. The temperature (Fig. 3b) is slightly increased with increasing ε_1 values. The entropy generation number is seen to be decreased with increasing values of ε_1.

Fig. 4 presents the distributions of velocity (f'), temperature (θ) and entropy generation number (N_G) with increasing ε_2. The velocity is elevated with increasing ε_2. A consistent acceleration in velocity is achieved for different ε_2 values (Fig. 4a). For greater values of ε_2, the viscosity of the fluid reduces and elasticity increases. Whereas, in Fig. 4b the temperature is reduced with increasing ε_2. Hence, the heat diffusion rate is decreased with increasing ε_2 values. In Fig. 4c it is seen that the entropy generation number is increased with increasing ε_2.

Fig. 5 illustrates the effects of velocity (f'), temperature (θ) and entropy generation number (N_G) distributions for increasing vales of S_f. A significant increase in velocity (Fig. 5a) is observed at the wall for increasing values of S_f. Hence, the momentum (velocity) boundary layer thickness will be increased. Similar trend were observed in [27, 43, 44] and [56]. In Fig. 5b, a monotonic decay in temperature is seen with increasing S_f. Therefore, the thermal boundary layer thickness is decreased. The N_G is slightly decreased with increasing S_f.

Fig. 6 presents the effects of velocity (f') temperature (θ) and entropy generation number (N_G) distributions for increasing thermal jump parameter, S_T. A considerable decrease in velocity, temperature and entropy generation number is observed with increasing S_T. The thermal slip parameter is inversely proportional to Grashof number, Gr. An increase in Gr, decelerates the boundary layer flow due to acceleration in buoyancy. An increase in thermal slip parameter, the Grashof number decreases. A similar trend was observed in [27, 43, 44] and [56].

Fig. 7 depict the impact of magnetic parameter M on velocity (f'), temperature (θ) and entropy generation number (N_G). The parameter M represents the ratio of magnetic Lorentzian drag force to viscous hydrodynamic force in the flow. For $M > 1$, the magnetic force dominates the viscous force hence the magnetohydrodynamic effect is strong. Thereby, the flow is controlled by the magnetic field. And for $M = 1$, the magnetic force and the viscous force are of same magnitude. An increase in M induces a marked deceleration in velocity (Fig. 7a). The radial magnetic field acts to generate a perpendicular drag force and hence decelerates the flow. In contrast, Fig. 7b indicates an elevation in temperature with increasing M values. A significant decrease in entropy generation number is seen with increasing M values.

Figs. 8–10 present the profiles for entropy generation number, N_G and Bejan number, Be, for different values of Re, Br, Ha and Ω. Both N_G and Be are boosted with increasing Re values, as seen in Figs. 8a and 8b, which is due to an increase in inertia force of the flow and reduction in viscous force. Figs. 9a and 9b present the influence of N_G and Be for variation in Br. In Fig. 8a, increasing Br is found to increase N_G. Br is defined as the ratio of viscous heat to external heating. Also Br

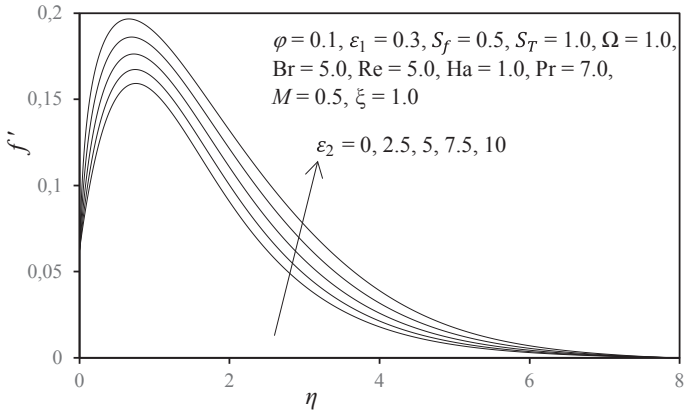

(a) Influence of ε_2 on velocity profiles

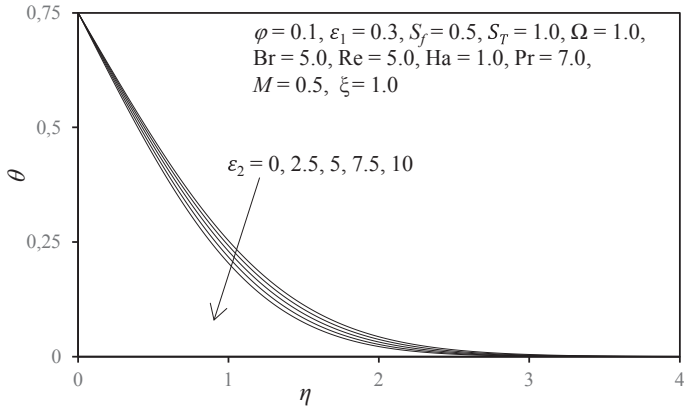

(b) Influence of ε_2 on temperature profiles

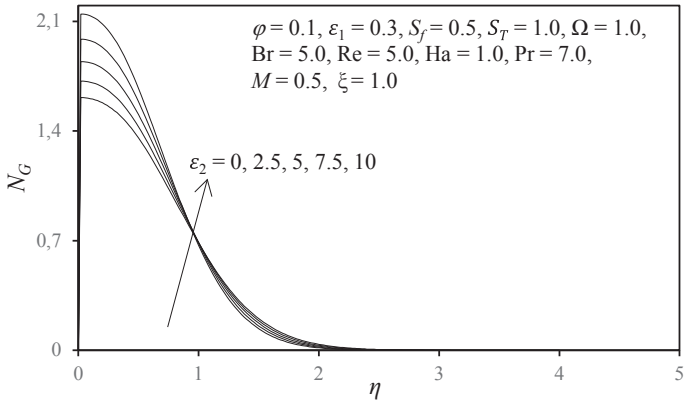

(c) Influence of ε_2 on entropy generation number

Fig. 4. Influence of ε_2 on various parameters

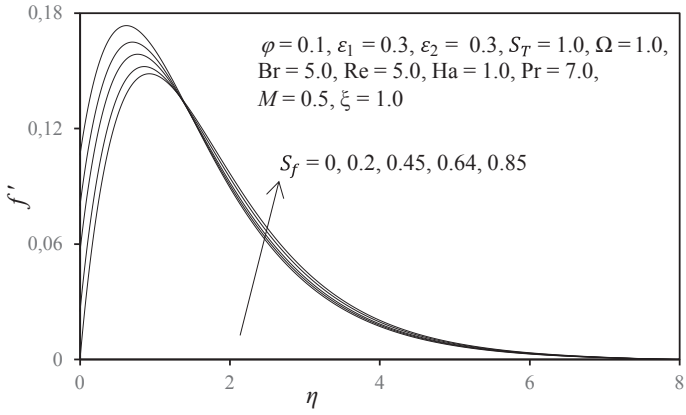

(a) Influence of S_f on velocity profiles

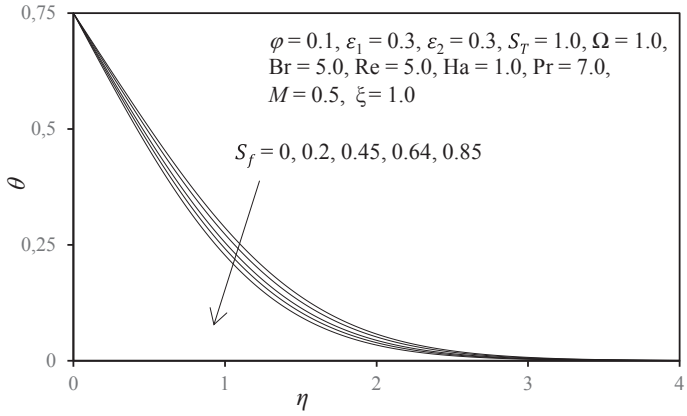

(b) Influence of S_f on temperature profiles

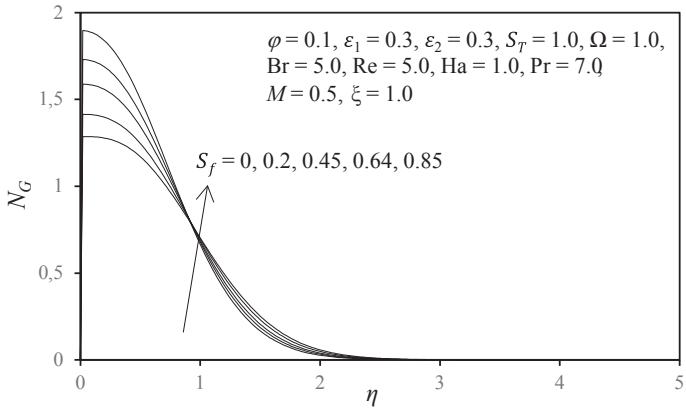

(c) Influence of S_f on entropy generation number

Fig. 5. Influence of S_f on various parameters

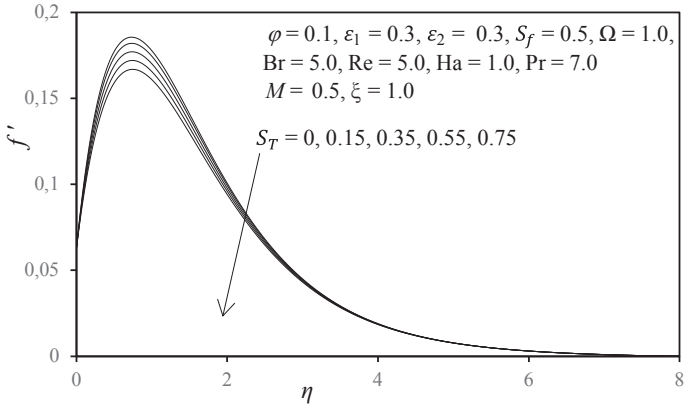

(a) Influence of S_T on velocity profiles

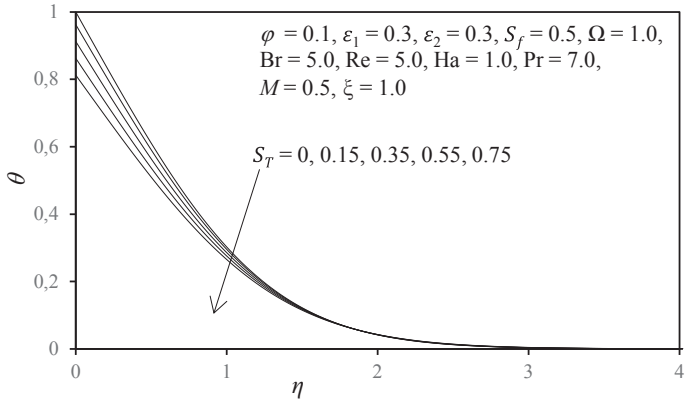

(b) Influence of S_T on temperature profiles

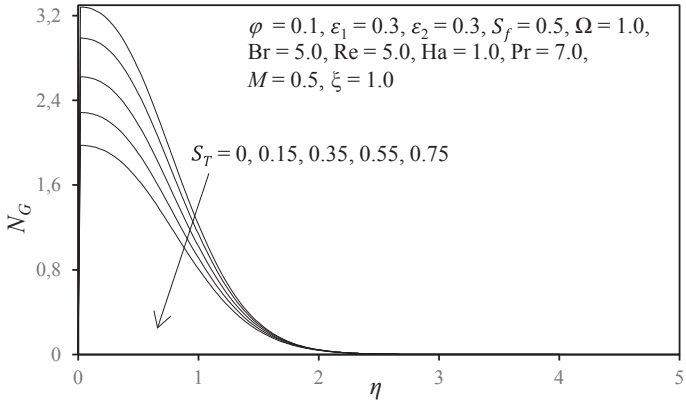

(c) Influence of S_T on entropy generation number

Fig. 6. Influence of S_T on various parameters

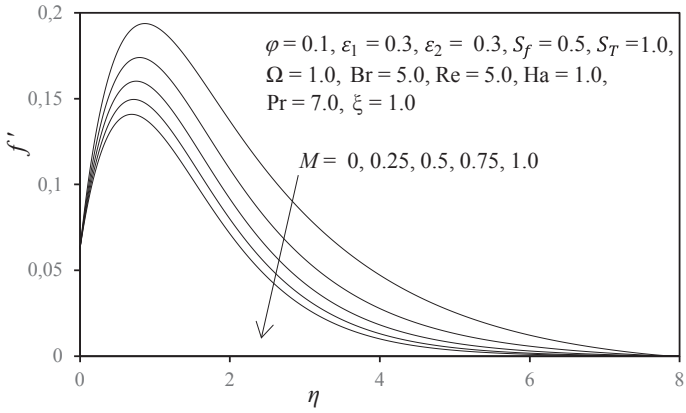

(a) Influence of M on velocity profiles

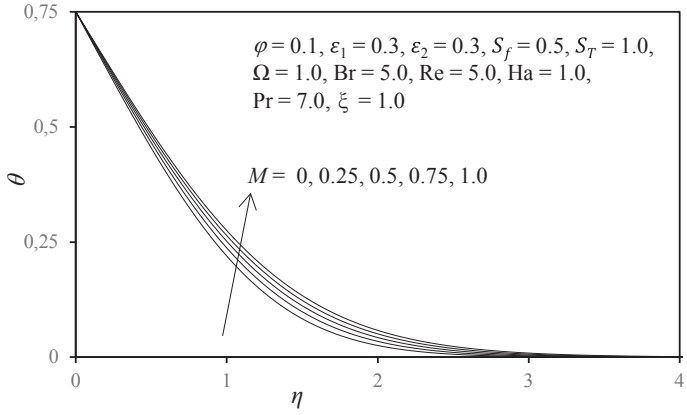

(b) Influence of M on temperature profiles

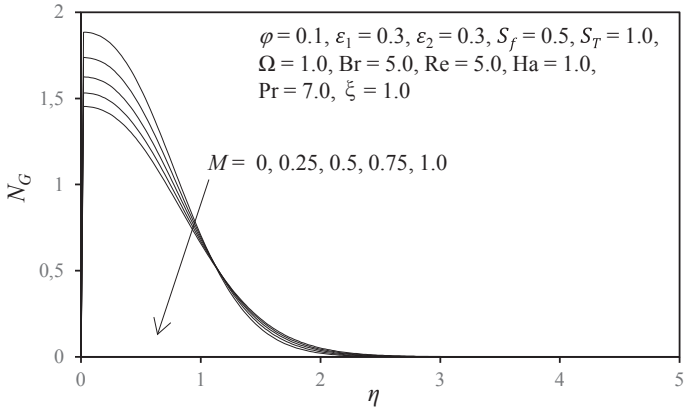

(c) Influence of M on entropy generation number

Fig. 7. Influence of M on various parameters

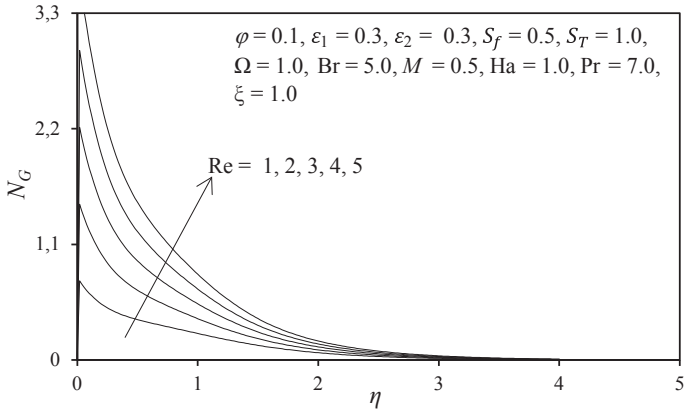

(a) Influence of Re on entropy generation number

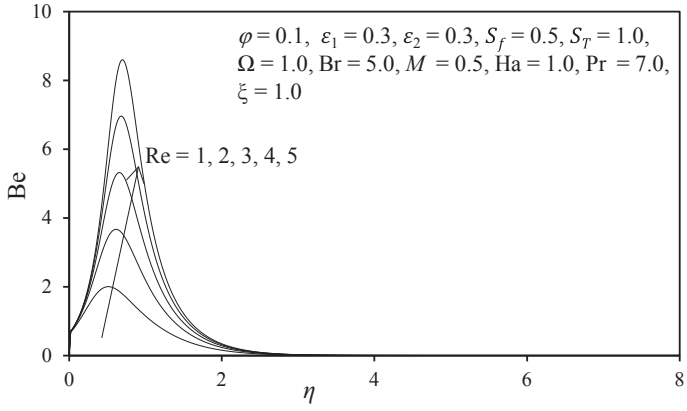

(b) Influence of Re on Bejan number

Fig. 8. Influence of Re on various parameters

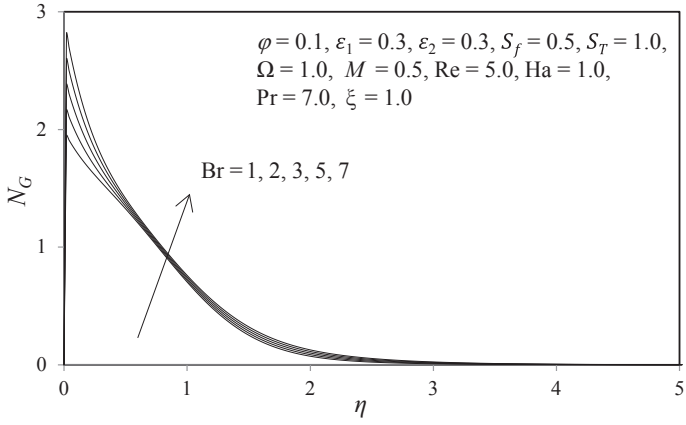

Fig. 9. (a) Influence of Br on entropy generation number

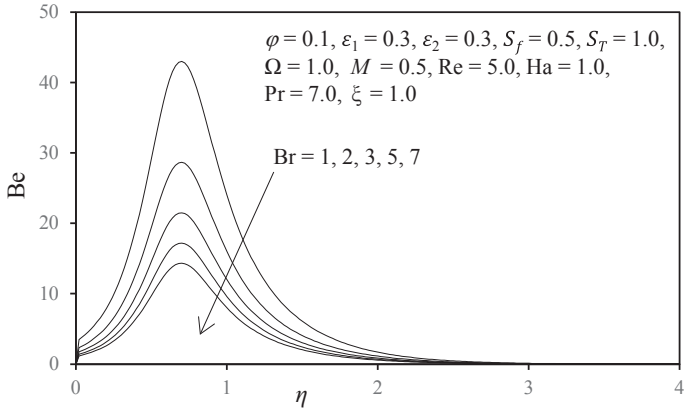

Fig. 9. (b) Influence of Br on Bejan number

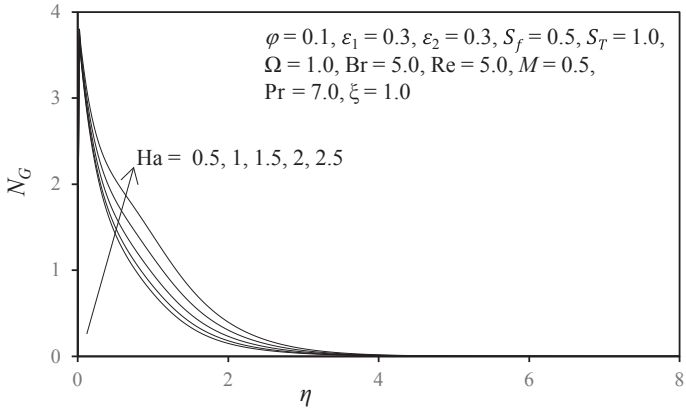

(a) Influence of Ha on entropy generation number

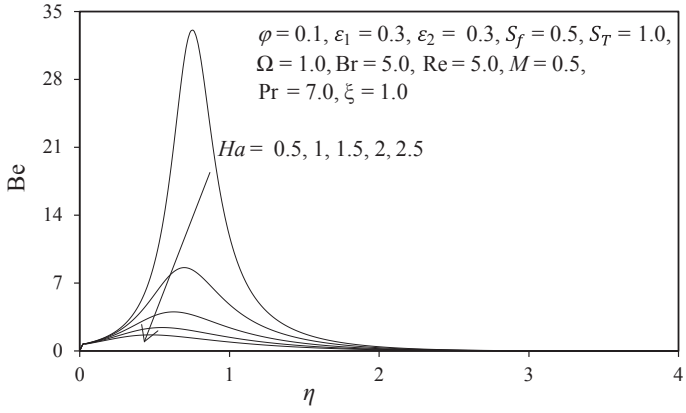

(b) Influence of Ha on Bejan number

Fig. 10. Influence of Ha on various parameters

is directly proportional to square of cylinder velocity. Therefore, as Br increases, a considerable increase in N_G is observed as shown in Fig. 9a. A significant decrease in Be is observed in Fig. 9a with an increase in Br. Similar effects were observed in [34]. The impacts of Ha on N_G and Be are presented in Figs. 10a and 10b. It is seen that an increasing Ha, increases N_G but reduces Be, which leads to an increase in the heat transfer irreversibility at the cylinder surface.

Figs. 11–12 visualize the streamlines for different values of third-grade fluid parameter, φ and magnetic parameter, M. Streamlines are used to visualize the

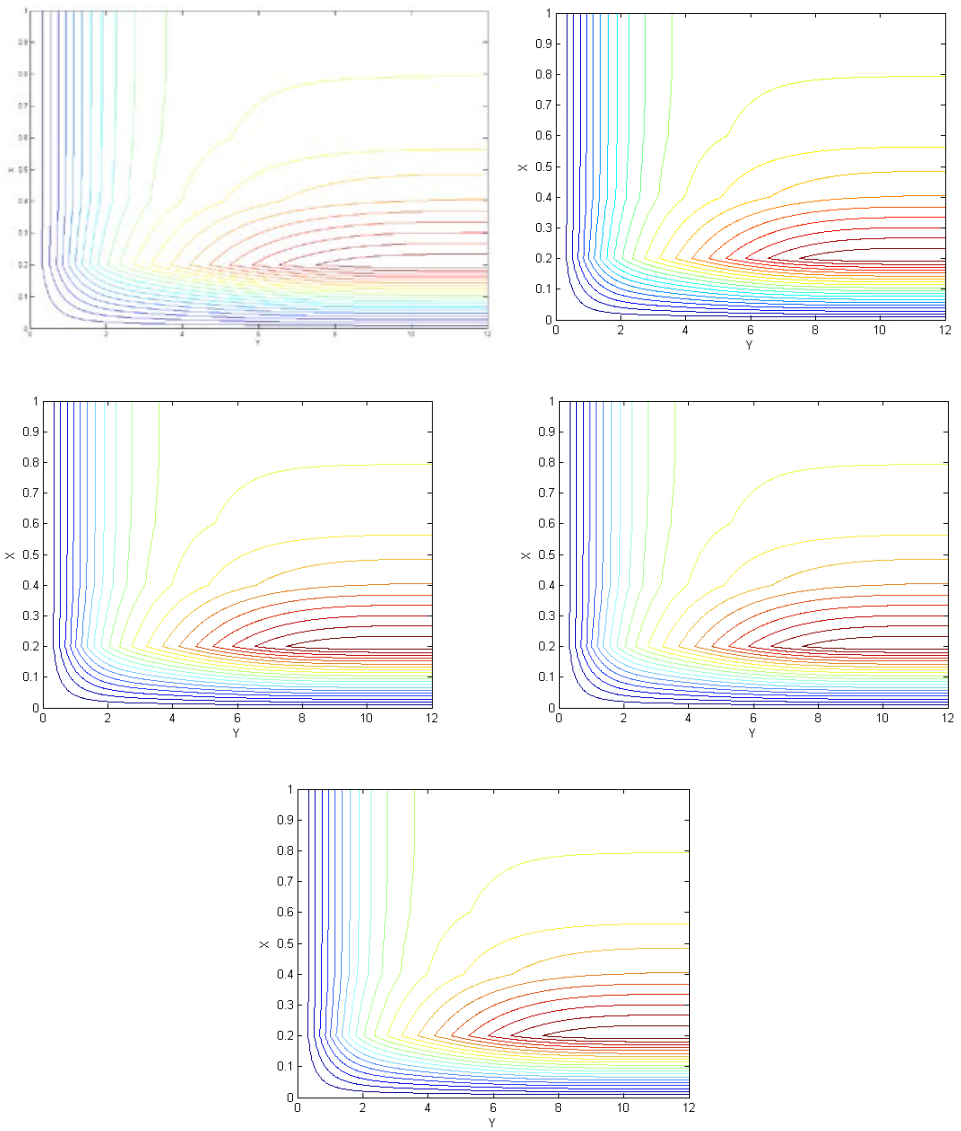

Fig. 11. Streamlines for various values of φ

fluid flow and the stream function. Also, streamlines define the flow behavior of the automotive design.

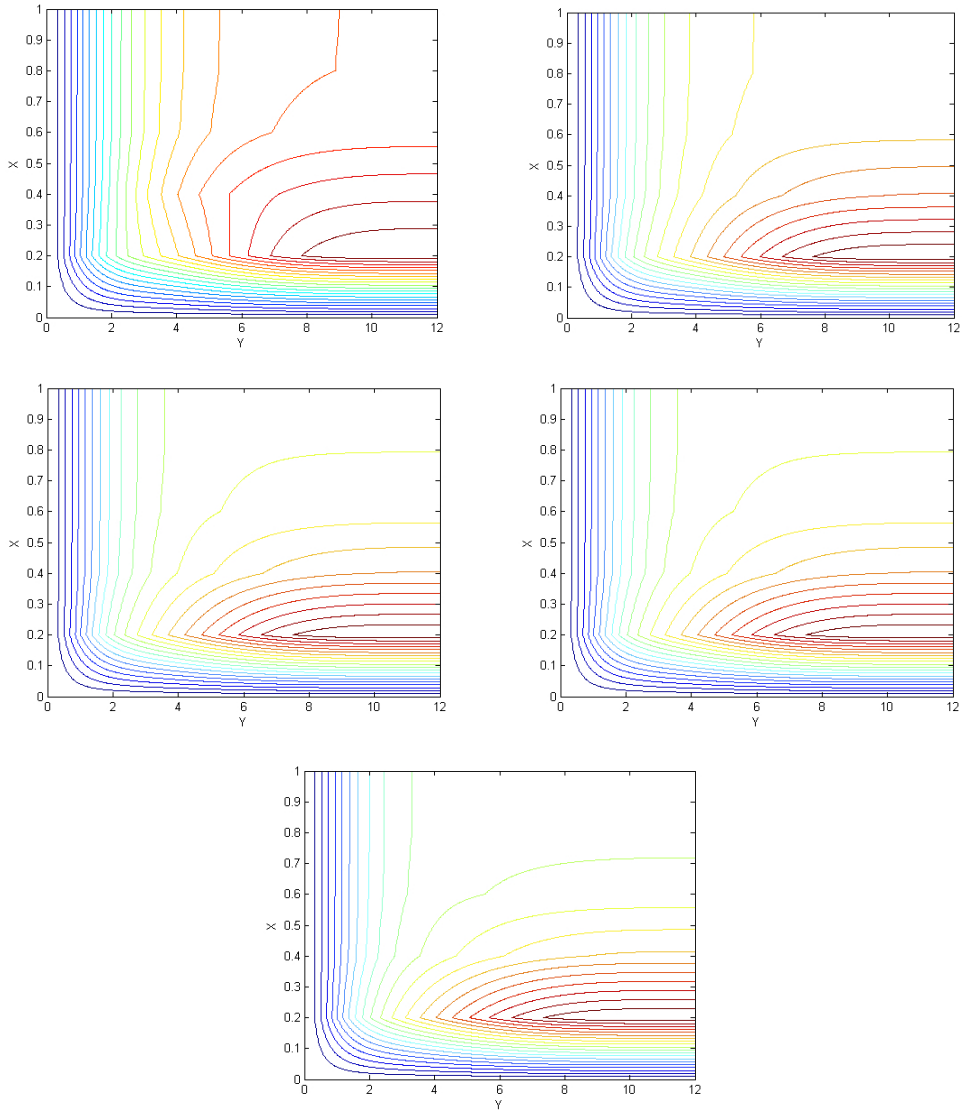

Fig. 12. Streamlines for various values of M

5. Conclusions

In this paper, the governing boundary layer equations are solved analytically by Keller-Box method. The effect of various thermophysical parameters on velocity and temperature are discussed numerically and presented graphically. The influence

of Reynolds number, Brinkman number, Hartmann number and dimensionless heat function on entropy generation number and Bejan number is also discussed. The streamlines are also presented. The present code is validated with the previous Newtonian case studies. The observations that include increasing φ, M and ε_1 are seen to decrease both the velocity and entropy generation number whereas the temperature is increased. Increasing ε_2 and S_f increases both the velocity and entropy generation number, but the temperature is reduced throughout boundary layer. Increasing S_T is seen to decrease velocity, temperature and entropy generation number.

Manuscript received by Editorial Board, May 06, 2018;
final version, August 08, 2018.

References

[1] T.F. Irvine and J. Karni. Non-Newtonian fluid flow and heat transfer. *Handbook of Single-Phase Convective Heat Transfer*, chapter 20, Wiley New York, 20.1–20.57, 1987.

[2] A. Borrelli, G. Giantesio, and M.C. Patria. MHD Oblique stagnation-point flow of a micropolar fluid. *Applied Mathematical Modelling*, 36(9):3949–3970, 2012. doi: 10.1016/j.apm.2011.11.004.

[3] A. Hussain and A. Ullah. Boundary layer flow of a Walter's B fluid due to a stretching cylinder with temperature dependent viscosity. *Alexandria Engineering Journal*, 55(4):3073–3080, 2016. doi: 10.1016/j.aej.2016.07.037.

[4] S.A. Gaffar, V.R. Prasad, and E.K. Reddy. Computational study of Jeffrey's non-Newtonian fluid past a semi-infinite vertical plate with thermal radiation and heat generation/absorption. *Ain Shams Engineering Journal*, 8(2):277–294, 2017. doi: 10.1016/j.asej.2016.09.003.

[5] A.S. Rao, C.H. Amanulla, N. Nagendra, O.A. Bég, and A. Kadir. Hydromagnetic flow and heat transfer in a Williamson non-Newtonian fluid from a horizontal circular cylinder with Newtonian heating. *International Journal of Applied and Computational Mathematics*, 3(4):3389–3409, 2017. doi: 10.1007/s40819-017-0304-x.

[6] V.R. Prasad, S.A. Gaffar, and O.A. Bég. Non-similar computational solutions for free convection boundary layer flow of a nanofluid from an isothermal sphere in a non-Darcy porous medium. *Journal of Nanofluids*, 4(2):203–213, 2015. doi: 10.1166/jon.2015.1149.

[7] H. Li and Y. Jian. Dispersion for periodic electro-osmotic flow of Maxwell fluid through a microtube. *International Journal of Heat and Mass Transfer*, 115:703–713, 2017. doi: 10.1016/j.ijheatmasstransfer.2017.07.065.

[8] S.A. Gaffar, V.R. Prasad, and O.A. Bég. Computational study of non-Newtonian Eyring-Powell fluid from a vertical porous plate with Biot number effects. *Journal of the Brazilian Society of Mechanical Sciences and Engineering*, 39(7):2747–2765, 2017. doi: https://doi.org/10.1007/s40430-017-0761-5.

[9] S.A. Gaffar, V.R. Prasad, and E.K. Reddy. Computational study of MHD free convection flow of non-Newtonian tangent hyperbolic fluid from a vertical surface in porous media with Hall/Ionslip current and Ohmic dissipation. *International Journal of Applied and Computational Mathematics*, 3(2):859–890, 2017. doi: 10.1007/s40819-016-0135-1.

[10] R. Mehmood, S. Rana, and S. Nadeem. Transverse thermophoretic MHD Oldroyd-B fluid with Newtonian heating. *Results in Physics*, 8:686–693, 2018. doi: 10.1016/j.rinp.2017.12.072.

[11] Z-Y. Xie and Y-J. Jian. Rotating electromagnetohydrodynamic flow of power-law fluids through a microparallerl channel. *Colloids and Surfaces A: Physicochemical and Engineering Aspects*, 529:334–345, 2017. doi: 10.1016/j.colsurfa.2017.05.062.

[12] T. Hayat, A. Shafiq, and A. Alsaedi. Effect of Joule heating and thermal radiation in flow of third grade fluid over radiative surface. *PLoS ONE* 9(1):e83153. doi: 10.1371/journal.pone.0083153.

[13] S.A. Gaffar, V.R. Prasad, O.A. Bég, Md. H.H. Khan, and K. Venkatadri. Radiative and magnetohydrodynamics flow of third-grade viscoelastic fluid past an isothermal inverted cone in the presence of heat generation/absorption. *Journal of the Brazilian Society of Mechanical Sciences and Engineering*, 40:127, 2018. doi: 10.1007/s40430-018-1049-0.

[14] A.T. Akinshile. Steady flow and heat transfer analysis of third grade fluid with porous medium and heat generation. *Engineering Science and Technology, an International Journal*, 20(6):1602–1609, 2017. doi: 10.1016/j.jestch.2017.11.012.

[15] N. Ahmed, S.U. Jan, U. Khan, and T.M. Syed. Heat transfer analysis of third-grade fluid flow between parallel plates: analytical solutions. *International Journal of Applied and Computational Mathematics*, 3(2):579–589, 2017. doi: 10.1007/s40819-015-0109-8.

[16] T. Hayat, A. Kiran, M. Imtiaz, A. Alsaedi, and M. Ayub. Melting heat transfer in the MHD flow of a third-grade fluid over a variable-thickness surface. *The European Physical Journal Plus*, 132:id265, 2017. doi: 10.1140/epjp/i2017-11519-4.

[17] K. Ayub, M. Yaqub Khan, M. Ashraf, J. Ahmad, and Q. Mahmood-Ul-Hassan. On some results of third-grade non-Newtonian fluid flow between two parallel plates. *The European Physical Journal Plus*, 132:id552, 2017. doi: 10.1140/epjp/i2017-11821-1.

[18] M.K. Nayak, S. Shaw, and A.J. Chamkha. Radiative non-linear heat transfer analysis on wire coating from a bath of third-grade fluid. *Thermal Science and Engineering Progress*, 5:97–106, 2018. doi: 10.1016/j.tsep.2017.11.001.

[19] G.J. Reddy, A. Hiremath, and M. Kumar. Computational modeling of unsteady third-grade fluid flow over a vertical cylinder: A study of heat transfer visualization. *Results in Physics*, 8:671–682, 2018. doi: 10.1016/j.rinp.2017.12.054.

[20] T. Hayat, S. Qayyum, A. Alsaedi, and B. Ahmad. Mechanisms of double stratification and magnetic field in flow of third grade fluid over a slendering stretching surface with variable thermal conductivity. *Results in Physics*, 8:819–828, 2018. doi: 10.1016/j.rinp.2017.12.057.

[21] K. Ahmad and A. Ishak. Magnetohydrodynamic (MHD) Jeffrey fluid over a stretching vertical surface in a porous medium. *Propulsion and Power Research*, 6(4):269–276, 2017. doi: 10.1016/j.jppr.2017.11.007.

[22] F.I. Alao, A.I. Fagbade, and B.O. Falodun. Effects of thermal radiation, Soret and Dufour on an unsteady heat and mass transfer flow of a chemically reacting fluid past a semi-infinite vertical plate with viscous dissipation. *Journal of Nigerian Mathematical Society*, 35(1):142–58, 2016. doi: 10.1016/j.jnnms.2016.01.002.

[23] K. Bhattacharyya and G.C. Layek. Magnetohydrodynamic boundary layer flow of nanofluid over an exponentially stretching permeable sheet. *Physics Research International*, 2014:id 592536, 2014. doi: 10.1155/2014/592536.

[24] Z-Y. Xie and Y-J. Jian. Entropy generation of two-layer magnetohydrodynamic electoosmotic flow through microparallel channels. *Energy*, 139:1080–1093, 2017. doi: 10.1016/j.energy.2017.08.038.

[25] S.A. Gaffar, V.R. Prasad, and E.K. Reddy. Magnetohydrodynamics flow of Non-Newtonian fluid from a vertical permeable cone in the presence of thermal radiation and heat generation/absorption. *International Journal of Applied and Computational Mathematics*, 3(4):2849–2872, 2017. doi: 10.1007/s40819-016-0262-8.

[26] S.A. Gaffar, V.R. Prasad, and E.K. Reddy. Magnetohydrodynamic free convection flow and heat transfer of non-Newtonian tangent hyperbolic fluid from horizontal circular cylinder with Biot number effects. *International Journal of Applied and Computational Mathematics*, 3(2):721–743, 2017. doi: 10.1007/s40819-015-0130-y.

[27] S.A. Gaffar, V.R. Prasad, and O.A. Bég. Computational analysis of magnetohydrodynamic free convection flow and heat transfer of non-Newtonian tangent hyperbolic fluid from a horizontal circular cylinder with partial slip. *International Journal of Applied and Computational Mathematics*, 1(4):651–675, 2015. doi: 10.1007/s40819-015-0042-x.

[28] S.A. Gaffar, V.R. Prasad, E.K. Reddy, and O.A. Bég. Magnetohydrodynamic free convection boundary layer flow of non-Newtonian tangent hyperbolic fluid from a vertical permeable cone with variable surface temperature. *Journal of Brazilian Society of Mechanical Sciences and Engineering*, 39(1):101–116, 2017. doi: 10.1007/s40430-016-0611-x.

[29] O.A. Bég, S.A. Gaffar, V.R. Prasad, and M.J. Uddin. Computational solutions for non-isothermal, nonlinear magneto-convection in porous media with Hall/Ionslip currents and Ohmic dissipation. *Engineering Science and Technology, an International Journal*, 19(1):377–394, 2016. doi: 10.1016/j.jestch.2015.08.009.

[30] A. Bejan. The concept of irreversibility in heat exchanger design: counter flow heat exchangers for gas-to-gas applications. *Journal of Heat Transfer*, 99(3):374–380, 1977. doi: 10.1115/1.3450705.

[31] M.G. Sobamowo and A.T. Akinshilo. Analysis of flow, heat transfer and entropy generation in a pipe conveying fourth grade fluid with temperature dependent viscosities and internal heat generation. *Journal of Molecular Liquids*, 241:188–198, 2017. doi: 10.1016/j.molliq.2017.05.145.

[32] M.M. Rashidi, S. Bagheri, E. Momoniat, and N. Freidoonimehr. Entropy analysis of convective MHD flow of third grade non-Newtonian fluid over a stretching sheet. *Ain Shams Engineering Journal*, 8(1):77–85, 2017. doi: 10.1016/j.asej.2015.08.012.

[33] S. Baag, S.R. Mishra, G.C. Dash, and M.R. Acharya. ntropy generation analysis for viscoelastic MHD flow over a stretching sheet embedded in a porous medium. *Ain Shams Engineering Journal*, 8(4):623–632, 2017. doi: 10.1016/j.asej.2015.10.017.

[34] T. Hayat, M.W. Ahmed Khan, M. Ijaz Khan, and A. Alsaedi. Nonlinear radiative heat flux and heat source/sink on entropy generation minimization rate. *Physica B: Condensed Matter*, 538:95–103, 2018. doi: 10.1016/j.physb.2018.01.054.

[35] M. Qasim, Z. Hayat Khan, Ilyas Khan, and Q.M. Al-Mdallal. Analysis of entropy generation in flow of methanol-based nanofluid in a sinusoidal wavy channel. *Entropy*, 19(10):490, 2017. doi: 10.3390/e19100490.

[36] P. Rana, N. Shukla, O.A. Bég, A. Kadir, and B. Singh. Unsteady electromagnetic radiative nanofluid stagnation-point flow from a stretching sheet with chemically reactive nanoparticles, Stefan blowing effect and entropy generation. *Proceedings of the Institution of Mechanical Engineers, Part N: Journal of Nanomaterials, Nanoengineering and Nanosystems*, 2018. doi: 10.1177/2397791418782030.

[37] S.E. Ahmed, M.A. Mansour, A. Mahdy, and S.S. Mohamed. Entropy generation due to double diffusive convective flow of Casson fluids over nonlinearity stretching sheets with slip conditions. *Engineering Science and Technology, an International Journal*, 20(6):1553–1562, 2017. doi: 10.1016/j.jestch.2017.10.002.

[38] E.M. Sparrow and S.H. Lin. Laminar heat transfer in tubes under slip-flow conditions. *Journal of Heat Transfer*, 84(4):363–369, 1962. doi: 10.1115/1.3684399.

[39] D. Srinivasacharya and K. Hima Bindu. Entropy generation in a porous annulus due to micropolar fluid flow with slip and convective boundary conditions. *Energy*, 111:165–177, 2016. doi: 10.1016/j.energy.2016.05.101.

[40] M.K. Nayak, S. Shaw, V.S. Pandey, and A.J. Chamkha. Combined effects of slip and convective boundary conditions on MHD 3D stretched flow of nanofluid through porous media inspired by non-linear thermal radiation. *Indian Journal of Physics*, 92(9):1017–1028, 2018. doi: 10.1007/s12648-018-1188-2.

[41] M. Qayyum, H. Khan, and O. Khan. Slip analysis at fluid-solid interface in MHD squeezing flow of Casson fluid through porous medium. *Results in Physics*, 7:732–750, 2017. doi: 10.1016/j.rinp.2017.01.033.

[42] D. Srinivasacharya and K. Himabindu. Effect of slip and convective boundary conditions on entropy generation in a porous channel due to micropolar fluid flow. *International Journal of Nonlinear Sciences and Numerical Simulation*, 19(1):11–24, 2018. doi: 10.1515/ijnsns-2016-0056.

[43] S.A. Gaffar, V.R. Prasad, E.K. Reddy, and O.A. Bég. Free convection flow and heat transfer of non-Newtonian tangent hyperbolic fluid form an isothermal sphere with partial slip. *Arabian Journal for Science and Engineering*, 39(11):8157–8174, 2014. doi: 10.1007/s13369-014-1310-5.

[44] S.A. Gaffar, V.R. Prasad, and O.A. Bég. Free convection flow and heat transfer of tangent hyperbolic fluid past a vertical porous plate with partial slip. *Journal of Applied Fluid Mechanics*, 9(4):1667–1678, 2016. doi: 10.18869/acadpub.jafm.68.235.24718.

[45] R.B. Bird, R.C. Armstrong, and O. Hassager. *Dynamics of Polymeric Liquids. Volume 1: Fluid Mechanics*. 2nd edition, Wiley Interscience, New York, 1987.

[46] R.G. Larson. *Constitutive Equations for Polymer Melts and Solutions*. Butterworths, Boston, 1988. doi: 10.1016/C2013-0-04284-3.

[47] C. Truesdell and W. Noll. *The Non-Linear Field Theories of Mechanics*. 3rd edition, Springer-Verlag, Berlin, 2004. doi: 10.1007/978-3-662-10388-3.

[48] H.B. Keller. Numerical methods in boundary-layer theory. *Annual Review of Fluid Mechanics*, 10:417–433, 1978. doi: 10.1146/annurev.fl.10.010178.002221.

[49] M.S. Abel, P.S. Datti, and N. Mahesha. Flow and heat transfer in a power-law fluid over a stretching sheet with variable thermal conductivity and non-uniform heat source. *International Journal of Heat and Mass Transfer*, 52(11–12):2902–2913, 2009. doi: 10.1016/j.ijheatmasstransfer.2008.08.042.

[50] S.A. Gaffar, V.R. Prasad, B.R. Kumar, and O.A. Bég. Computational modelling and solutions for mixed convection boundary layer flows of nanofluid from a non-isothermal wedge. *Journal of Nanofluids*, 7(5):1024–1032,2018. doi: 10.1166/jon.2018.1522.

[51] S.A. Gaffar, V.R. Prasad, E.K. Reddy, and O.A. Bég. Thermal radiation and heat generation/absorption effects on viscoelastic double-diffusive convection from an isothermal sphere in porous media. *Ain Shams Engineering Journal*, 6(3):1009–1030, 2015. doi: 10.1016/j.asej.2015.02.014.

[52] Y.L. Zhang and K. Vairavamoorthy. Analysis of transient flow in pipelines with fluid–structure interaction using method of lines. *International Journal for Numerical Methods in Engineering*, 63(10):1446–1460, 2005. doi: 10.1002/nme.1306.

[53] S.A. Gaffar, V.R. Prasad, and E.K. Reddy. MHD free convection flow of Eyring-Powell fluid from vertical surface in porous media with Hall/Ionslip currents and Ohmic dissipation. *Alexandria Engineering Journal*, 55(2):875–905, 2016. doi: 10.1016/j.aej.2016.02.011.

[54] J.H. Merkin. Free convection boundary layers on cylinders of elliptic cross section. *Journal of Heat Transfer*, 99(3):453–457, 1977. doi: 10.1115/1.3450717.

[55] K.A. Yih. Effect of blowing/suction on MHD-natural convection over horizontal cylinder: UWT or UHF. *Acta Mechanica*, 144(1–2):17–27, 2000. doi: 10.1007/BF01181825.

[56] C.H. Amanulla, N. Nagendra, and M.S. Reddy. Numerical simulation of slip influence on electric conducting viscoelastic fluid past an isothermal cylinder. *Frontiers in Heat and Mass Transfer*, 10, 10, 2018. doi: 10.5098/hmt.10.10.